

Article

Unusual Catalytic Effect of Fe³⁺ on 2,4-dichlorophenoxyacetic Acid Degradation by Radio Frequency Discharge in Aqueous Solution

Yongjun Liu * and Bing Sun

College of Environmental Science & Engineering, Dalian Maritime University, Dalian 116026, China; sunb88@dmlu.edu.cn

* Correspondence: lyjglow@dmlu.edu.cn; Tel.: +86-411-847-252-75; Fax: +86-411-847-276-70

Abstract: 2,4-dichlorophenoxyacetic acid (2,4-D) is a widely used herbicide for controlling broad-leaved weeds. The development of an efficient process for treating the refractory 2,4-D wastewater is necessary. In this study, liquid-phase degradation of 2,4-D induced by radio frequency discharge (RFD) was studied. Experimental results showed that the degradation was more effective in acidic than in neutral or alkaline solutions. During the degradation, a large amount of hydrogen peroxide (H₂O₂, 1.2 mM/min, almost equal to that without 2,4-D) was simultaneously produced, and catalytic effects of both ferric (Fe³⁺) and ferrous (Fe²⁺) ions on the degradation were examined and compared. It was found that 2,4-D degraded more rapidly in the case of Fe³⁺ than the that of Fe²⁺. Such a scenario is explained that Fe³⁺ was successively reduced to Fe²⁺ by the atomic hydrogen (•H) and •OH-adducts of 2,4-D resulting from RFD, which in turn catalyzed the H₂O₂ to form more •OH radicals through Fenton's reaction, indicating that Fe³⁺ not only accelerates the degradation rate but also increases the amount of •OH available for 2,4-D degradation by suppressing the back reaction between the •H and •OH. 2,4-dichlorophenol, 4,6-dichlororesorcinol, 2-hydroxy-4-chloro- and 2-chloro-4-hydroxy- phenoxyacetic acids, hydroxylated 2,4-Ds, and carboxylic acids (glycolic, formic and oxalic) were identified as the byproducts. Energy yields of RFD have been compared with those of other nonthermal plasma processes.

Keywords: aqueous solution; radio frequency discharge; 2,4-D; degradation; Fenton



Citation: Liu, Y.; Sun, B. Unusual Catalytic Effect of Fe³⁺ on 2,4-dichlorophenoxyacetic Acid Degradation by Radio Frequency Discharge in Aqueous Solution. *Water* **2022**, *14*, 1719. <https://doi.org/10.3390/w14111719>

Academic Editors: Cassan Hodaifa, Antonio Zuorro, Joaquín R. Dominguez, Juan García Rodríguez, José A. Peres and Zacharias Frontistis

Received: 2 May 2022
Accepted: 23 May 2022
Published: 27 May 2022

Publisher's Note: MDPI stays neutral with regard to jurisdictional claims in published maps and institutional affiliations.



Copyright: © 2022 by the authors. Licensee MDPI, Basel, Switzerland. This article is an open access article distributed under the terms and conditions of the Creative Commons Attribution (CC BY) license (<https://creativecommons.org/licenses/by/4.0/>).

1. Introduction

2,4-dichlorophenoxyacetic acid (2,4-D) is a systemic herbicide extensively used for broad-leaved weeds control in cereal crops, pastures, and orchards. 2,4-D kills dicots (but not grasses) by mimicking the growth hormone auxin, causing uncontrolled growth and eventual death of the susceptible plants [1]. In 2015, the International Agency for Research on Cancer (IARC) confirmed its 1987 classification of 2,4-D as a Group 2B carcinogen [2,3]. Due to its massive use and high solubility in water, 2,4-D can easily seep into the aquatic environment during its production and application. 2,4-D is hardly biodegradable at concentrations higher than 1.0 mg/L [4]. Acid-washed powdered activated carbon (PAC) can effectively adsorb 2,4-D from aqueous media [5]. However, as PAC adsorption is just a phase transferring process, the adsorbent becomes a hazardous waste when it is saturated with pollutants that need to be properly disposed of. In this context, some energetic methods such as TiO₂ photocatalysis [6], electrochemical oxidation [7], gamma irradiation [8], sonolysis or their combination [9] have been developed. Although showing some promising, these processes suffer respective deficiencies of either process complexity or low energy utilization, and the search for efficient and effective 2,4-D decomposition processes is necessary.

In the past decades, electrical discharges for water purification have been investigated extensively [10–12]. Pulsed corona discharge (PCD) inside water, glow discharge in contact

with water and dielectric barrier discharge (DBD) close to water surface etc. were usually employed for the decomposition of harmful pollutants [12]. Degradation of 2,4-D by PCD over water surface [13,14] and by DBD in planar falling film reactor [15] have been evaluated and compared with some typical water treatment technologies. Recently, radio frequency discharge (RFD) [16,17] is receiving increasing attention as a novel plasma water treatment process due to its easy formation both in pure water and in solution with high conductivity [17], low breakdown voltage [18] and experimental simplicity. Several chemically active radicals ($\bullet\text{OH}$, $\text{H}\bullet$, $\bullet\text{O}$, etc.) derived from H_2O molecules were in situ generated, which can initiate the degradation of organic pollutants such as methylene blue [16] and Congo Red [18]. Wang et al. investigated the RFD of metronidazole [19] and found that reducing species played a significant role during the degradation. The formation of hydrogen peroxide (H_2O_2) during RFD of pure water was reported, and some catalytic effects of ferrous sulfate on the dye discoloration were observed. However, H_2O_2 quantification with the presence of the dye was not performed. In addition, when ferrous ion (Fe^{2+}) was added to the solution, it would be rapidly oxidized by H_2O_2 into ferric ion (Fe^{3+}) [16]. However, at present, no comparison in catalytic effect between Fe^{2+} and Fe^{3+} has been made. In this study, both 2,4-D degradation and H_2O_2 formation were investigated. Besides optimizing the experimental conditions, the catalytic mechanism of iron salts, especially that of the Fe^{3+} on the degradation was fully explored.

2. Experimental

The experimental apparatus, consisting of a radio frequency power supply (RSG-300, Reshige Electronics Inc., Changzhou, China), a vacuum matching box, a quartz reactor and a coaxial electrode system, is shown in Figure 1.

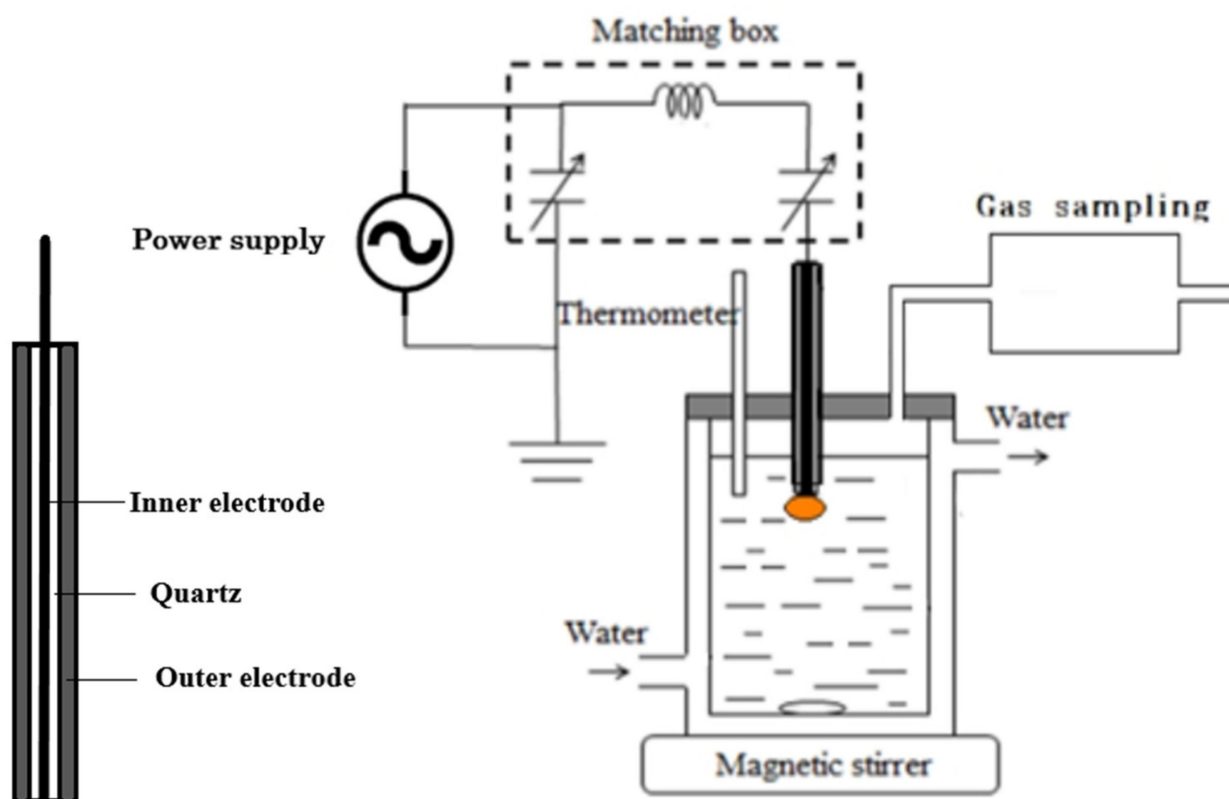


Figure 1. Experimental apparatus for 2,4-D degradation.

The reactor was a quartz cylinder with 60 mm of inner diameter and 150 mm in height. The coaxial electrode system consists of an inner electrode (pointed Pt wire, $\Phi = 1.0$ mm),

a quartz tube (i. d. = 1.0 mm, o. d. = 2.0 mm), and an outer electrode (copper tube, i. d. = 2.2 mm, o. d. = 3.0 mm). Discharge is generated at the tip of the inner electrode in contact with the liquid. In such an electrode system, the discharge can be stably sustained without the shielding box needed in conventional RFD [18,19]. 2,4-D was dissolved in distilled water and a 250 mL portion was poured into the reactor for treatment. Na₂SO₄ was used to adjust the solution conductivity. The pH of the solution was adjusted with dilute H₂SO₄ or NaOH to the expected value. During the reaction, the plasma heats the water in the reaction cell [16]. The reaction vessel was coated by a water jacket, where the temperature of the solution was kept at 298 ± 2K by running with cooling water.

During the discharge, the solution in the reactor was constantly agitated by a magnetic stirrer and the aliquots were periodically taken out for analysis. 2,4-D and the phenolic byproducts were analyzed by a reversed-phase HPLC (SHIMADZU LC-20A) coupled with a diode array UV detector. A C18 (4.6 × 25 mm) column was used for the separation. The eluent was composed of 40% acetonitrile and 59.9% H₂O and 0.1% H₃PO₄. The flow rate was 1.0 mL/min. The detection wavelength was usually set at 283 nm. Removal of 2,4-D ($\eta_{2,4-D}$) was calculated according to Equation (1).

$$\eta_{2,4-D}(\%) = \frac{(C_0 - C_t)}{C_0} \times 100 \quad (1)$$

where C_t (mM) was the concentration of 2,4-D at discharge time t and C_0 (mM) was the initial concentration of 2,4-D. Energy yields for 2,4-D removal ($J_{2,4-D}$) is calculated as Equation (2) [11,14].

$$J_{2,4-D} = \frac{C_0 Vol}{2Pt_{1/2}} \quad (2)$$

where Vol represents the solution volume (L), P the input power (W) and $t_{1/2}$, the discharge time required for 50% removal of 2,4-D (s).

The phenolic byproducts were identified by comparison of their retention times and UV spectra with those of the authentic standard samples or with the help of LC-MS [20]. Determination of organic acids and chloride ions (Cl⁻) was performed by ion chromatography (IC, DIONEX ICS-1100) equipped with an Ion Pac AG-23 column. 0.01 mol/L KOH solution was used as the eluent with a flow rate of 1.0 mL/min. H₂O₂ was determined by a colorimetric method where the yellow color pertitanic acid formed by mixing the treated solution with titanium sulfate was determined by absorption at 410 nm [21]. The concentration of Fe²⁺ was determined colorimetrically where 1,10-phenanthroline was used as the color reagent [22]. It is noted that some catalase should be immediately added to the solution to decompose the residue H₂O₂ as it interferes with the determination of the Fe²⁺. Total organic carbon (TOC) was measured by a TOC analyzer. The gaseous hydrogen evolved from the solution was determined by gas chromatography (GC-2014C, SHIMADZU). Each determination was performed three times and the average value was adopted, with a standard deviation of less than 4.5%.

3. Results and discussion

3.1. 2,4-D Degradation and Chloride Formation

2,4-D undergoes efficient degradation when subjected to RFD. Figure 2 shows the decays of 2,4-D and TOC and the formation of Cl⁻ during the RFD treatment.

As depicted in Figure 2, both 2,4-D and TOC declined exponentially while the yield of Cl⁻ increased gradually with increasing discharge time. The TOC decreased less rapidly than 2,4-D, indicating that intermediate byproducts were formed during the discharge. At the initial stage (<60 min), the yield of Cl⁻ is less than that expected from the decomposition of the parent compound. With 60 min of discharge treatment, 61% of 2,4-D was degraded and 0.32 mM of Cl⁻ was generated, meaning that only 26% of the organic chlorine of the transformed 2,4-D was mineralized into Cl⁻. After 140 min of discharge, the concentration of 2,4-D was below the detection limit and 1.63 mM of Cl⁻ was generated, where the yield

of Cl^- reached 82%. After 210 min, the Cl^- reached its stoichiometric point (2.0 mM), and after 300 min. (not shown in the figure), the concentration of TOC reached zero, indicating that 2,4-D was totally transformed into inorganic carbon and Cl^- under the action of RFD.

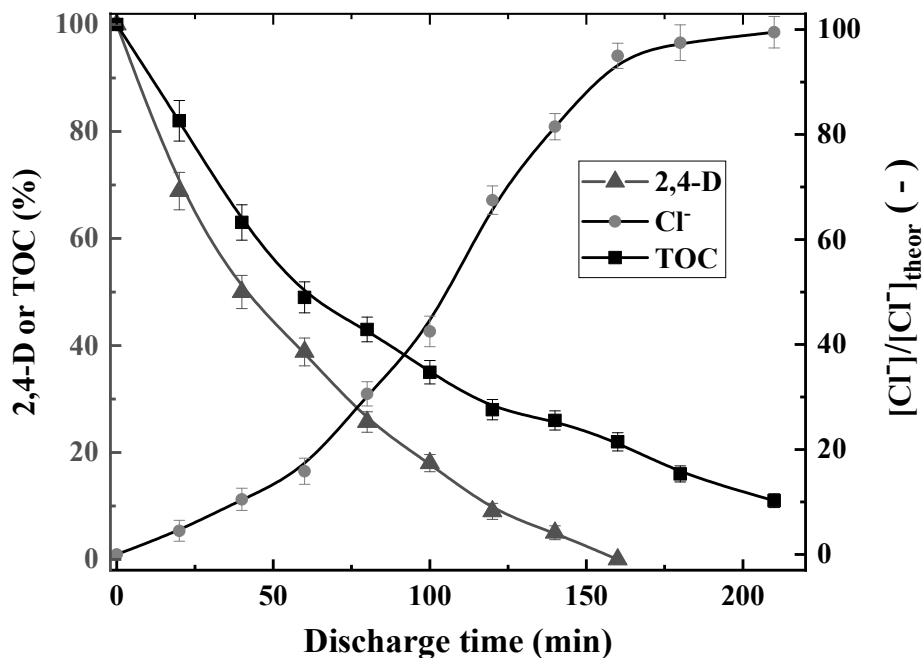


Figure 2. Decays of 2,4-D and TOC and formation of Cl^- during RFD treatment. ($[\text{2,4-D}]_0$, 1.0 mM; input power, 200 W; pH_0 , 6.51).

3.2. Effects of Initial pH on 2,4-D Degradation

pH is an important parameter affecting the degradation process. In order to better elucidate the effects of pH on 2,4-D degradation, pH variations during the RFD in the presence and absence of 2,4-D are illustrated in Figure 3.

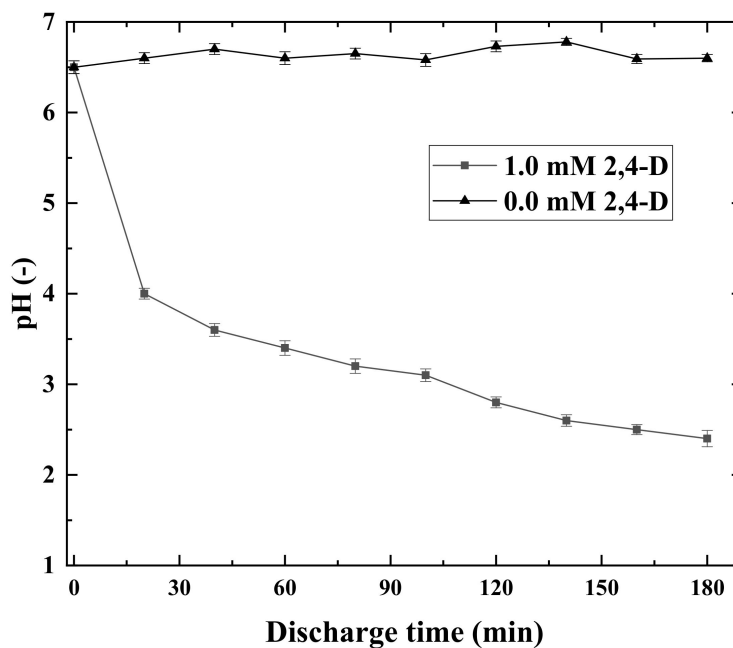


Figure 3. Variations of pH in the presence and absence of 2,4-D during RFD treatment (input power, 200 W; $[\text{2,4-D}]_0$, 1.0 mM; initial pH, 6.51).

As shown in Figure 3, without 2,4-D, the solution pH varied little during the discharge. However, in the presence of 2,4-D, the pH dropped dramatically. The decrease of pH in presence of 2,4-D can be explained by the formation of HCl and organic acids (*c.f.* 3.4). In order to better examine the effect and mechanism of pH on 2,4-D degradation, the experiments were performed both in buffered and unbuffered solutions. Here, phosphates were chosen as the buffering agents as the rate constants for the reactions of phosphates with $\bullet\text{OH}$ (e.g., Equations (3) and (4)) [23] are much smaller than that for the reaction of SO_4^{2-} (Equation (5)) [14].

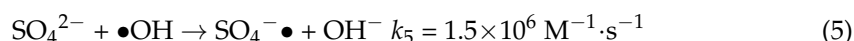
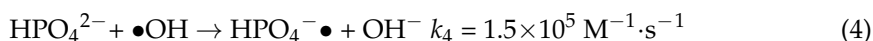
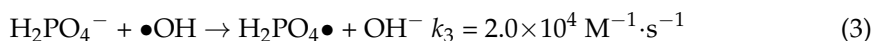


Figure 4 shows the 2,4-D removal under different initial pH (pH_0) values with 10 min of RFD treatment in unbuffered and phosphate buffered (prepared with 2.0 mM NaH_2PO_4 , no data from pH_0 3.0 to 6.0 as it has little buffering in the range) solutions.

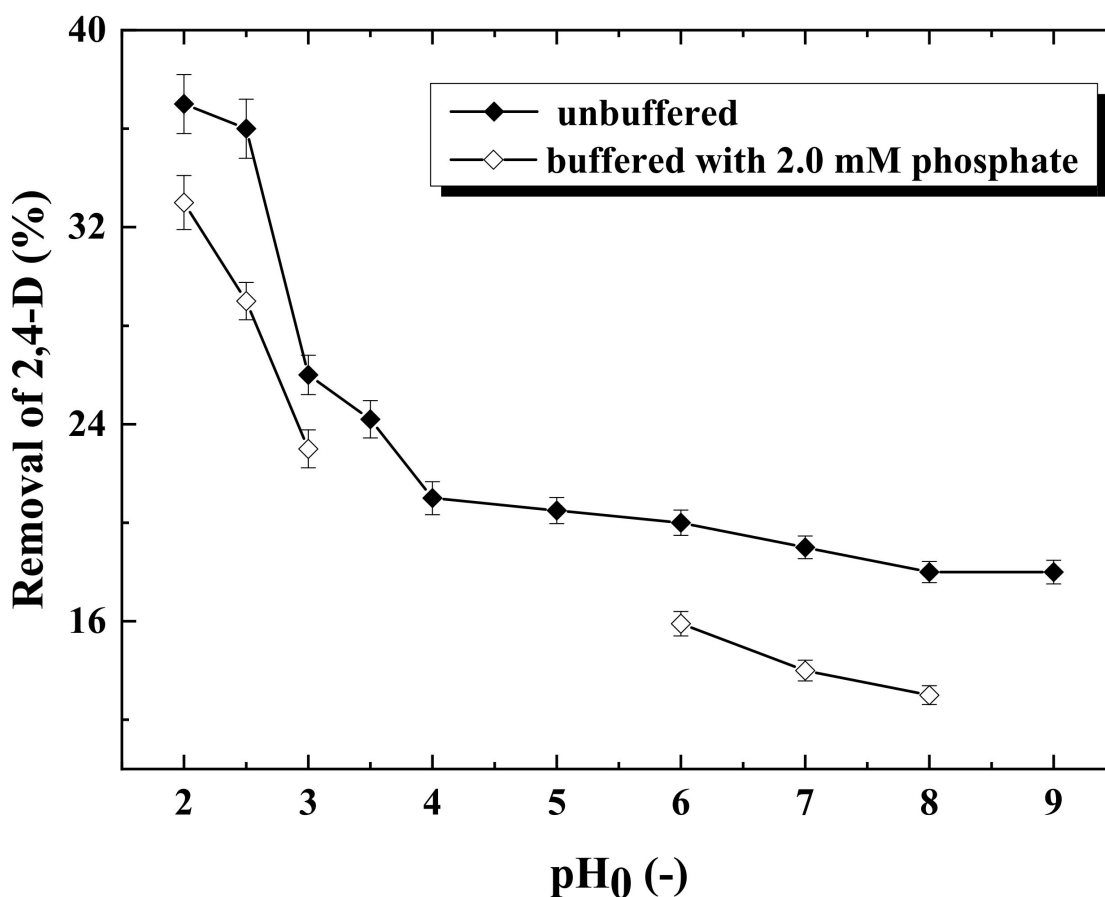
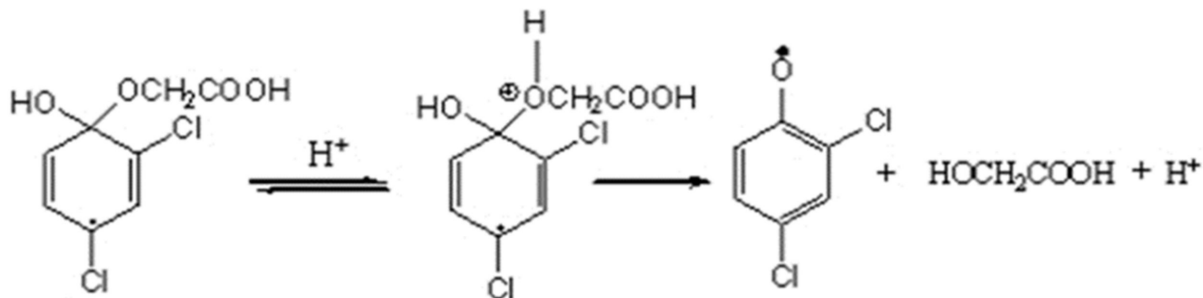


Figure 4. 2,4-D removal under different initial pH values in buffered and unbuffered solutions (input power, 200 W; $[\text{2,4-D}]_0$, 1.0 mM; discharge time, 10 min).

It can be observed from Figure 4 that the 2,4-D removal decreases with increasing pH_0 , both in the cases of the buffered and the unbuffered solutions. The removal of 2,4-D declined from 37% at pH_0 2.0 to almost half (18%) at pH_0 9.0 and from 33% at pH_0 2.0 to 13% at pH_0 8.0, meaning that the decrease is more pronounced in the buffered solution. Such phenomena can be explained that the degradation of 2,4-D in RFD is mainly an $\bullet\text{OH}$ radical process (degradation rate decreased in the presence of $\cdot\text{OH}$ scavenger, not shown in

the figure), [20] it is more advantageous to the decomposition under acidic conditions as the alkoxy group is more easily to be released from the C1 ·OH adducts in the presence of H^+ [24,25] (Scheme 1):



Scheme 1. H^+ catalyzed cleavage of C1 ·OH adducts.

Figure 4 shows that the difference in 2,4-D degradation between pH 4.0 and 9.0 was less noticeable in the case of unbuffered solution than in buffered ones, possibly due to the formation of acids which reduced the pH gap in the unbuffered system.

3.3. H_2O_2 Formation and Effects of Iron Salts on 2,4-D Degradation

Previous studies showed that the major molecular product formed in the liquid phase is H_2O_2 . [16,17] However, the formation of H_2O_2 in the presence of organic pollutants has rarely been reported. [16] In this investigation, H_2O_2 generated both in the presence and absence of 2,4-D is presented in Figure 5.

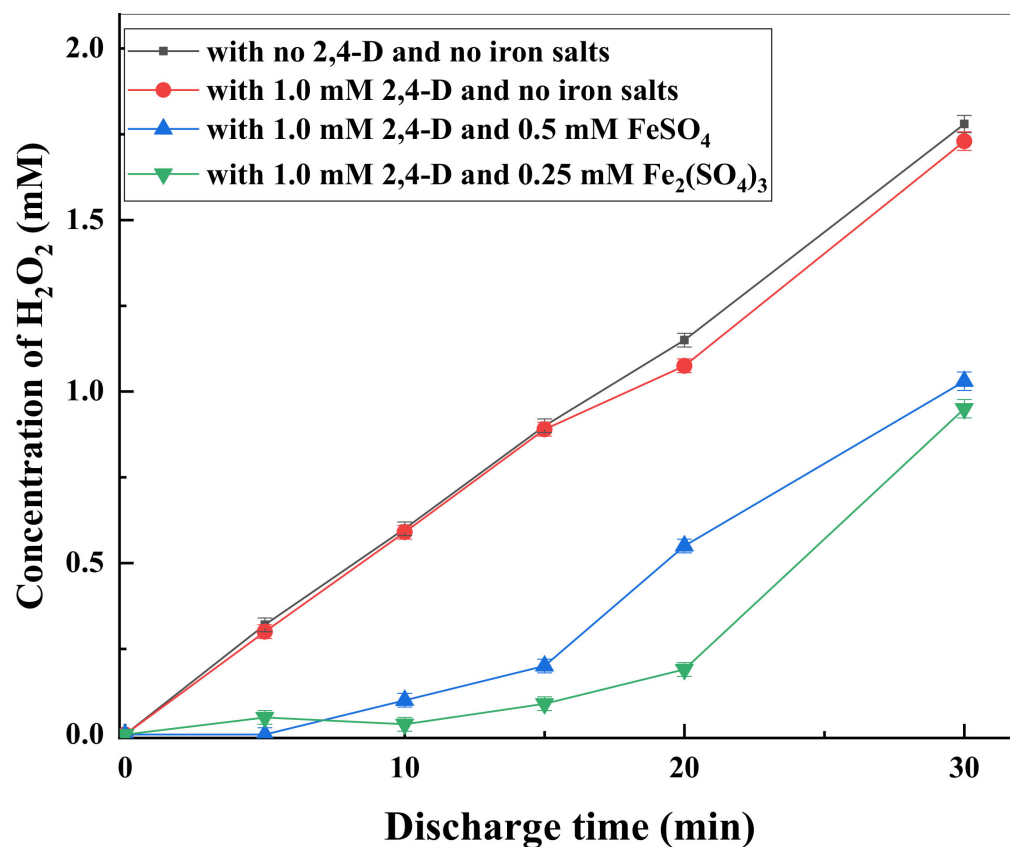
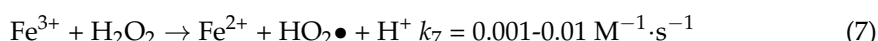
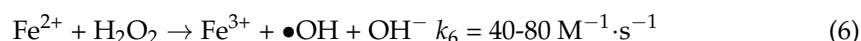


Figure 5. H_2O_2 generation in the presence and absence of 2,4-D in RFD (input power, 200 W; $[2,4-D]_0$, 1.0 mM; pH_0 , 5.6).

It can be seen in Figure 5 that less H_2O_2 was generated in 2,4-D solution than in solution without it, meaning that $\bullet\text{OH}$ radicals are the primary precursors of H_2O_2 and are the active species for 2,4-D degradation. However, the discrepancy is little in the early stage (<15 min), and the gap between the two concentrations of H_2O_2 was less than 10%, meaning that the concentration of $\bullet\text{OH}$ radicals near the plasma is so high that only a small part of them was consumed by 2,4-D and the rest dimerized to form H_2O_2 .

The concentration of H_2O_2 in the presence of 2,4-D traces the curve for experiments in its absence, indicating that H_2O_2 alone cannot lead to rapid degradation of 2,4-D. It is desirable to convert H_2O_2 into reactive $\bullet\text{OH}$ radicals for pollutant degradation. It is desirable to add iron ions to enhance the $\bullet\text{OH}$ radical formation and increase the 2,4-D decomposition through Fenton's reaction (Reactions (6) and (7)) [26].



The 2,4-D degradation in the presence of 0.5 mM iron ions is shown in Figure 6.

It can be observed from Figure 6 that both Fe^{2+} and Fe^{3+} showed remarkable catalytic effects on 2,4-D degradation. With 5 min of discharge, 2,4-D removal in the presence of Fe^{3+} (38%) was a little higher than that of Fe^{2+} (36%), where it was only 20% without a catalyzer. However, the catalytic effect of Fe^{3+} was more obvious than that of Fe^{2+} with increasing discharge time. At 10 min. the 2,4-D was totally removed in Fe^{3+} while only 70% was achieved for Fe^{2+} . Such a phenomenon is abnormal in conventional Fenton reactions, as the reaction (7) is several orders of magnitude slower than the reaction (6). The reason may be that Fe^{3+} has been reduced by the $\bullet\text{OH}$ -adducts formed by addition to the ring at positions unoccupied by the substituted groups (hydroxycyclohexadienyl radicals), producing the corresponding hydroxylated 2,4-Ds and Fe^{2+} [25,27] (Scheme 2):

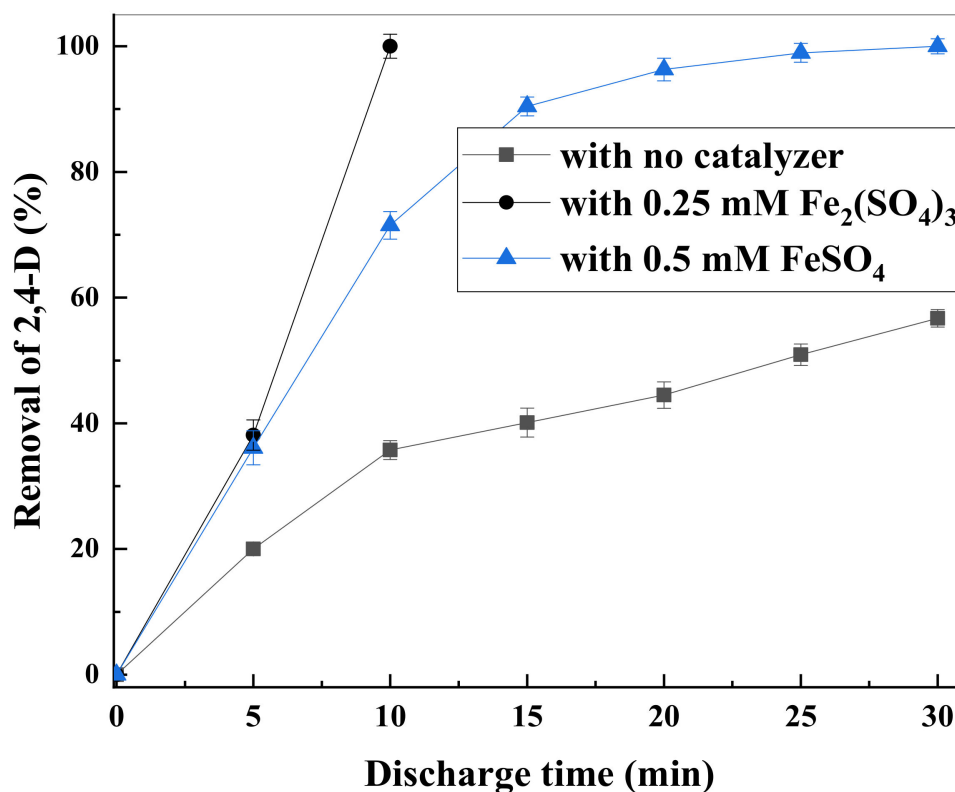
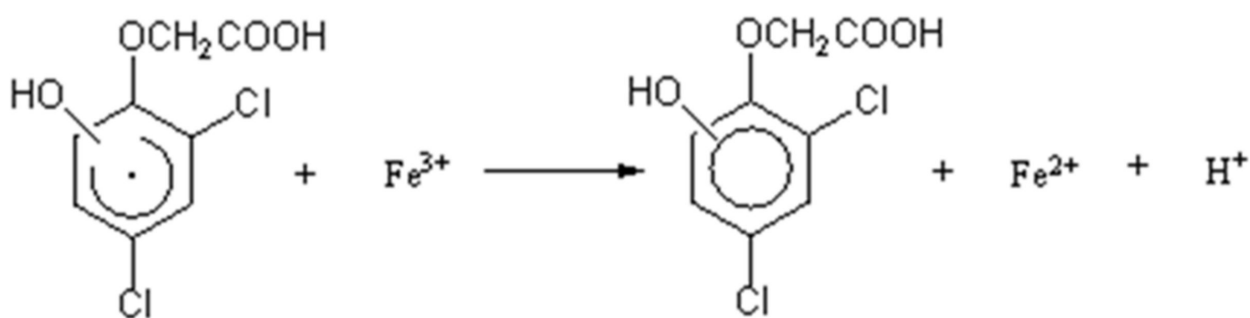


Figure 6. Effect of iron ions on 2,4-D removal in RFD treatment. (Conductivity 1.5 mS/cm, pH_0 2.0, input power 200 W).



Scheme 2. Fe^{3+} reduction by $\bullet\text{OH}$ -adducts formed by addition to the ring at positions unoccupied by the substituted groups (hydroxycyclohexadienyl radicals).

On the other hand, in the present pH range, much of Fe^{3+} is present in the form of FeOH^{2+} , which can be efficiently reduced by the $\cdot\text{H}$ atoms generated by the RFD to Fe^{2+} [28]:



Fe^{2+} ion resulting from the reactions above reacts with H_2O_2 (reaction (6)) to convert the H_2O_2 back to $\cdot\text{OH}$ radicals, ultimately leading to the decrease in H_2O_2 formation (Figure 5) and the increase in 2,4-D degradation (Figure 6) [13].

In order to prove the above assumptions, formations of Fe^{2+} and molecular hydrogen (H_2) during RFD were investigated, and the results were shown in Figure 7a and b, respectively.

It can be observed from Figure 7a that, in the case of Fe^{3+} , a lot of Fe^{2+} was formed during the RFD in the presence of 2,4-D and little Fe^{2+} was detected in the absence of 2,4-D, indicating the UV radiation from RFD is too weak to effectively induce the photoFenton activation ($\text{FeOH}^{2+} + \text{UV} \rightarrow \text{Fe}^{2+} + \cdot\text{OH}$) [29]. Figure 7b shows that the amount of H_2 in the gas phase decreased in the presence of Fe^{3+} . At 10 min. about 0.3 mmol H_2 was evolved from the solution in the absence of Fe^{3+} . However, only 0.19 mmol H_2 was detected when 0.5 mM Fe^{3+} was added to the solution, which means that at least 0.22 mmol Fe^{3+} was reduced to Fe^{2+} by the $\cdot\text{H}$ atoms. As the reaction between $\cdot\text{H}$ and $\cdot\text{OH}$ is suppressed due to the scavenging effect of Fe^{3+} [30], which in turn increases the amount of $\cdot\text{OH}$ radicals available for 2,4-D degradation.



However, as shown in Figure 7b, the amount of H_2 formed with the case of Fe^{2+} is higher than that without it. This can be explained that the $\bullet\text{OH}$ produced by RFD can rapidly oxidize the Fe^{2+} to Fe^{3+} , which suppressed the Reaction (9) and increase the amount of $\cdot\text{H}$ and ultimately the amount of H_2 via dimerization [30].



Fenton reagent ($\text{Fe}^{2+} + \text{H}_2\text{O}_2$) oxidation is an effective method for degradation of the refractory organic pollutants. However, the reaction has to be undertaken in acidic conditions (pH: 2–4). In addition, as the Fenton reaction proceeds, the Fe^{2+} rapidly oxidizes to Fe^{3+} and the reaction becomes a Fenton-like one, which leads to a substantial decrease in the reaction rate. In order to accelerate the reaction, ultraviolet light (UV) was usually employed (UV/Fenton). However, UV/Fenton was only effective in solutions with high UV transmittance. In RFD of 2,4-D, Fe^{3+} showed an extraordinary catalytic effect due to its successive reduction to the Fe^{2+} , meaning that RFD may be used to promote the Fenton-like reactions, especially in liquids with poor UV transmittance, which is of interest because most real wastewater is UV opaque. In addition, the pH of the solution can spontaneously

drop to the Fenton's operation range, indicating that Fe^{3+} /RFD is a promising process for 2,4-D degradation. In order to further clarify the potential application of RFD in accelerating the Fenton-like process, concentrated 2,4-D degradation by $\text{Fe}^{3+}/\text{H}_2\text{O}_2$ in the presence and absence of RFD was performed, and the results were shown in Figure 8.

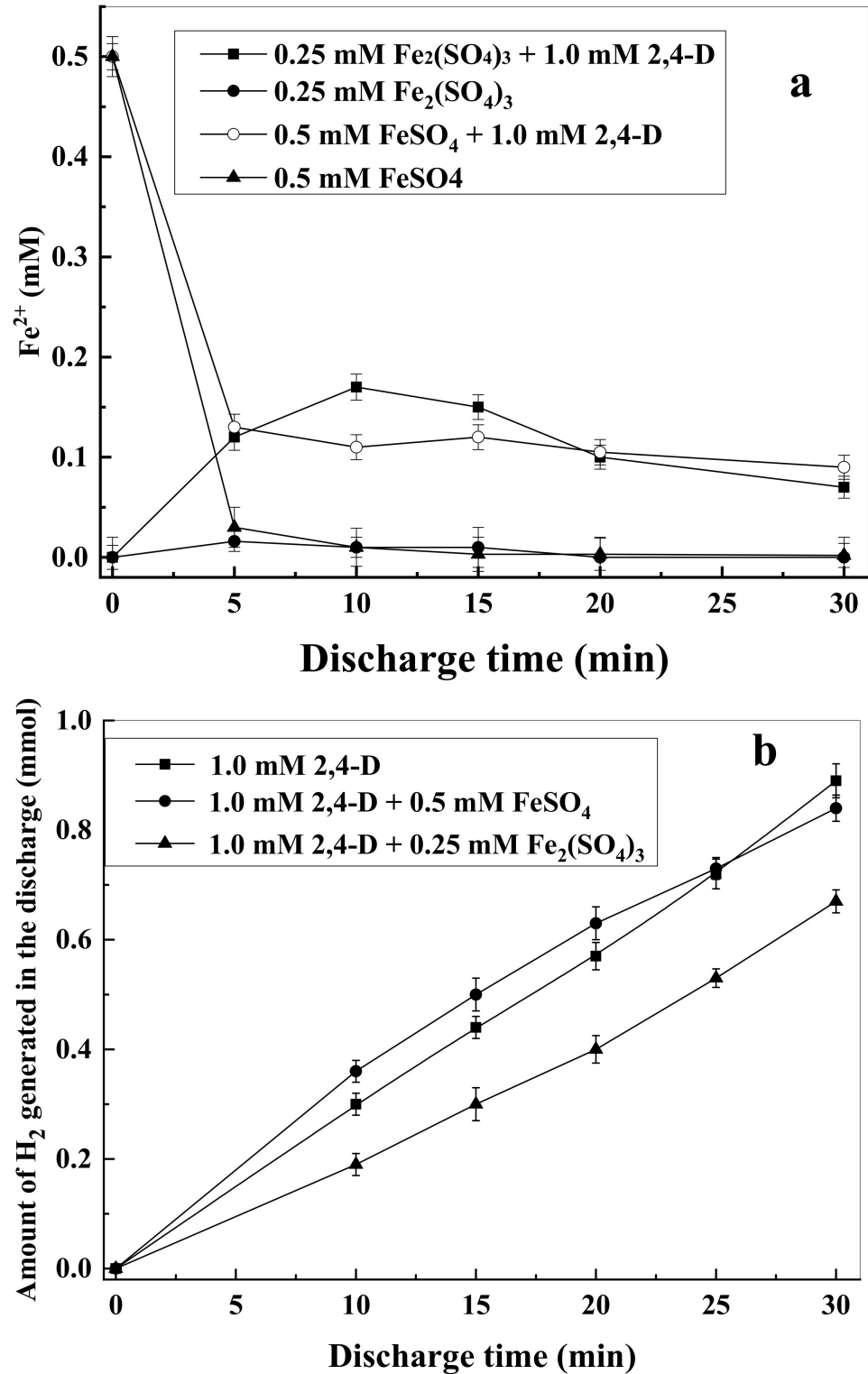


Figure 7. Formations of Fe^{2+} (a) and H_2 (b) during RFD (input power, 200 W; pH_0 , 2.0).

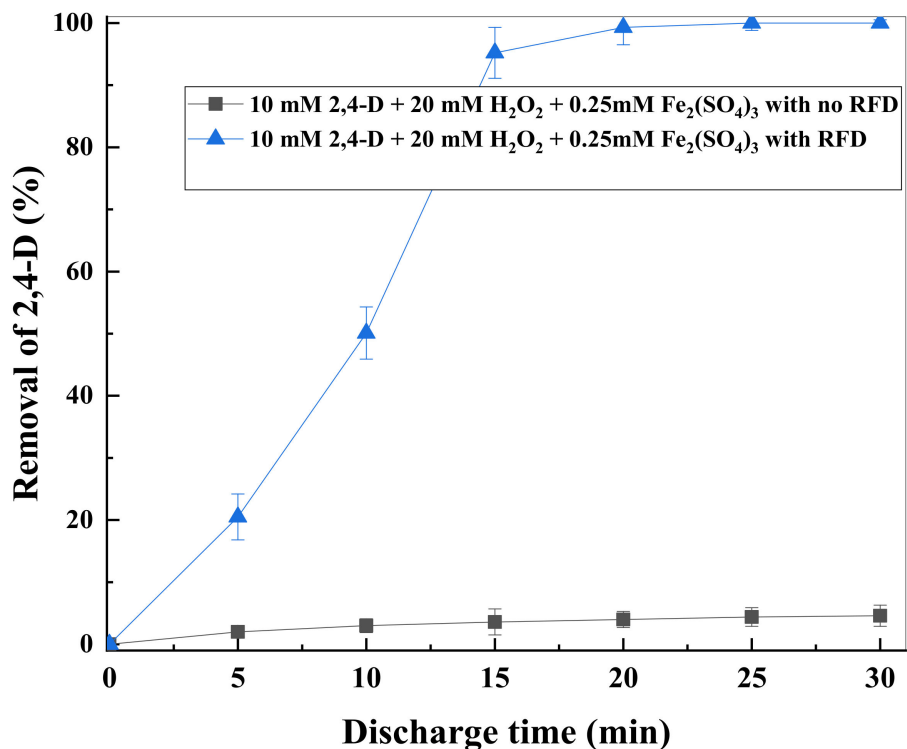


Figure 8. Accelerating effect of RFD for Fenton-like process (input power, 200 W; pH₀, 2.0).

It can be observed from Figure 8 that without RFD, little 2,4-D degradation proceeded. When RFD was applied in the Fenton-like process, the 2,4-D degradation was significantly enhanced where it could be removed completely in 25 min. of RFD, indicating that RFD was a useful tool for accelerating the Fenton-like process.

3.4. Intermediate Products Formation and Possible Decomposition Pathway

In order to gain insight into the 2,4-D decomposition mechanism, HPLC and IC were utilized to help identify the intermediate products. Figure 9 shows the HPLC chromatograms of the solution within 40 min of RFD treatment monitored at 283 nm.

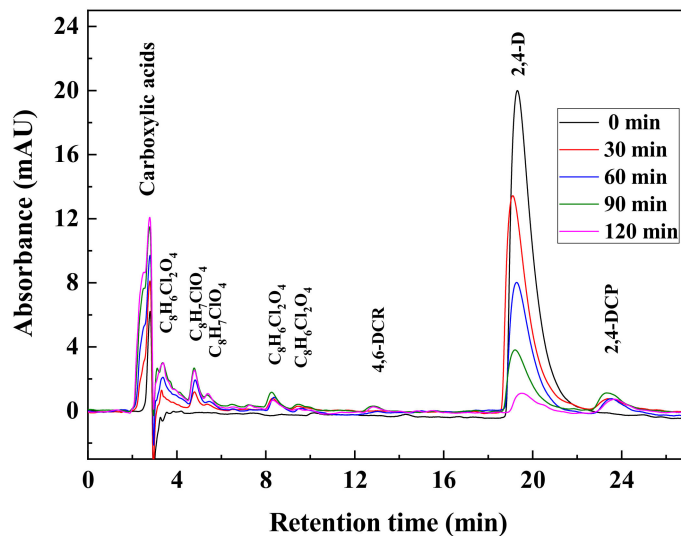


Figure 9. HPLC chromatograms during the RFD treatment (input power, 200 W; [2,4-D]₀, 1.0 mM; pH₀, 2.0).

As shown in Figure 9, several byproducts were observed. The peaks at retention times 12.8 min and 23.5 min are 4,6-dichlororesorcinol (4,6-DCR) and 2,4-Dichlorophenol (2,4-DCP), respectively. Three isomers of hydroxylation products of 2,4-D, i.e., 3-, 5- and 6-hydroxy-2,4-D ($C_8H_6Cl_2O_4$) and two chlorohydroxyl isomers (2-hydroxy-4-chloro- and 2-chloro-4-hydroxyphenoxyacetic acid: $C_8H_7ClO_4$) were roughly identified by the LC-MS [20]. As no standards are available for these products, their precise identification and quantification cannot be performed. As 2,4-DCP is found as a common intermediate byproduct in other methods, [6–9] the concentration variation of 2,4-DCP as a function of discharge time is given in Figure 10.

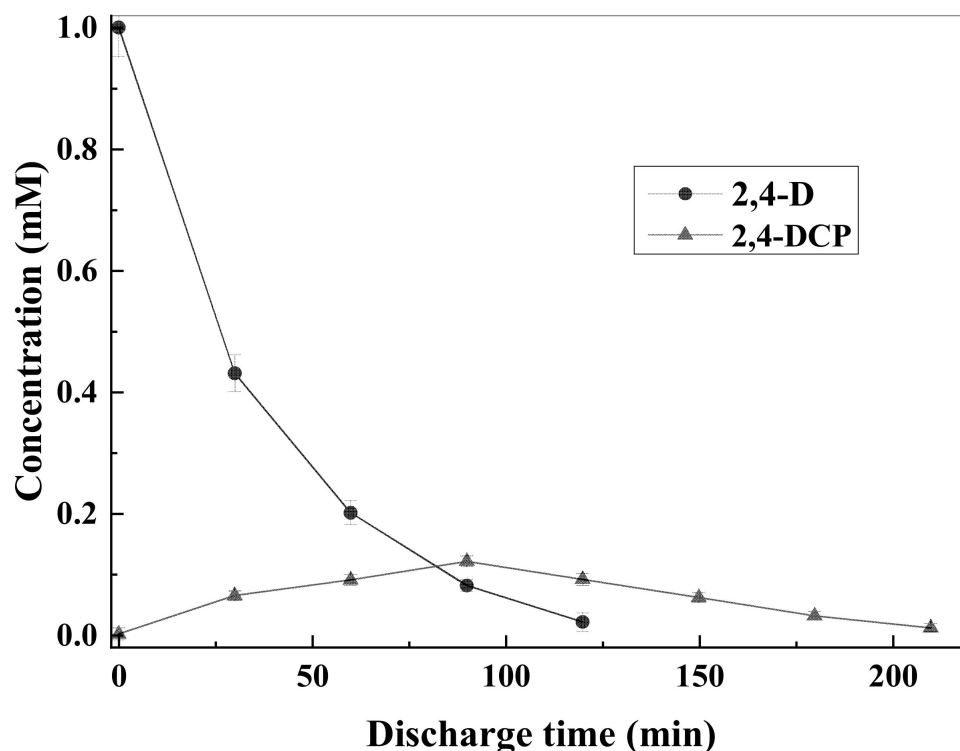


Figure 10. Appearance and decay profile of 2,4-DCP during RFD (input power, 200 W; $[2,4-D]_0$, 1.0 mM; pH_0 , 2.0).

It can be observed from Figure 10 that the 2,4-DCP forms immediately after the discharge takes place. Its concentration increases gradually with discharge time through to 90 min and then progressively diminishes. Such a gradual increasing and then decreasing trend is always observed in other treatment processes. The maximum concentration of 2,4-DCP formed is 0.11 mM in RFD of 1.0 mM 2,4-D. In comparison, more than 0.5 mM 2,4-DCP was formed in TiO_2 photocatalysis of 1.0 mM 2,4-D [6], 0.04 mM in γ radiolysis of 0.5 mM 2,4-D [8] and 0.02 mM in sonolysis of 0.22 mM of 2,4-D [9], respectively, indicating that the 2,4-DCP buildup/decomposition pattern in RFD is similar to those in γ radiolysis and sonolysis (the maximum concentration of 2,4-DCP is about 10% of the parent compound).

Aliphatic acids with a retention time of less than 3 min are difficult to quantify as HPLC cannot separate them well. Therefore, IC was employed to determine the organic acids, and results are shown in Figures 11 and 12, respectively.

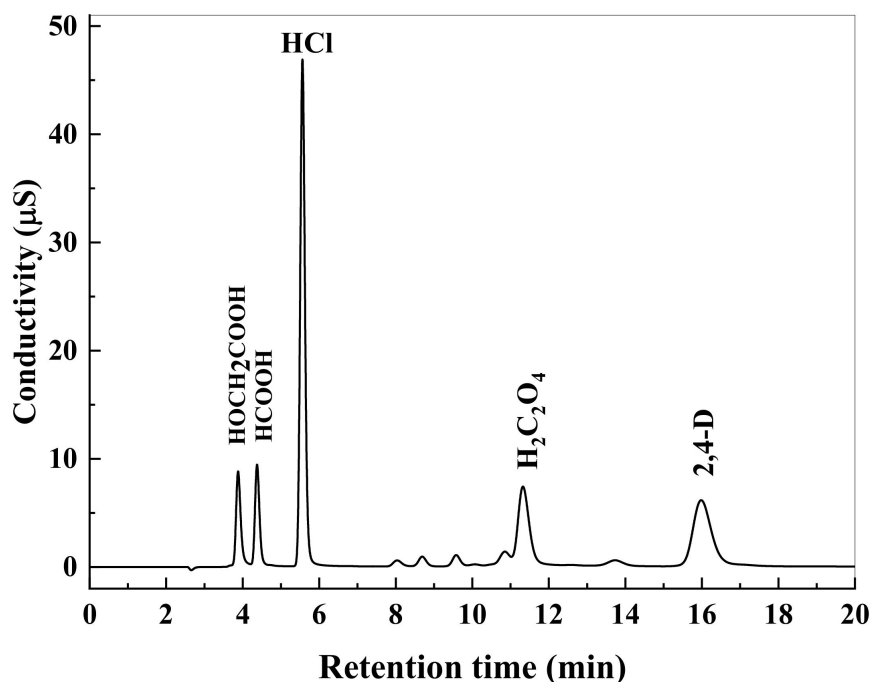


Figure 11. IC chromatogram of the RFD of 1.0 mM 2,4-D in pure water (input power, 200 W; discharge time, 40 min).

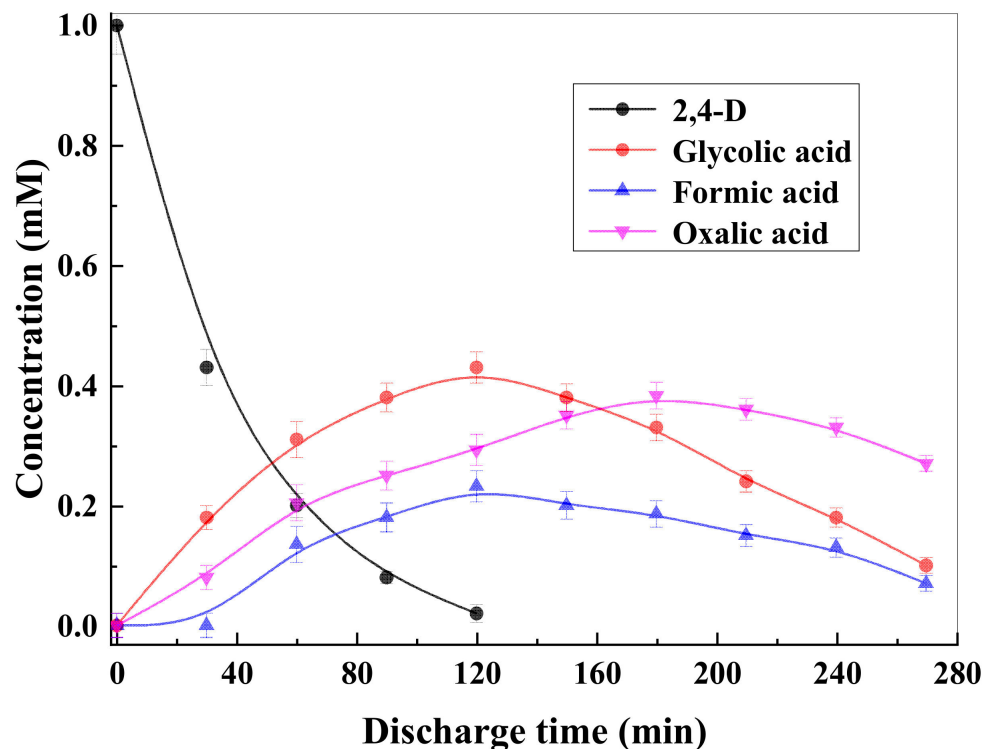
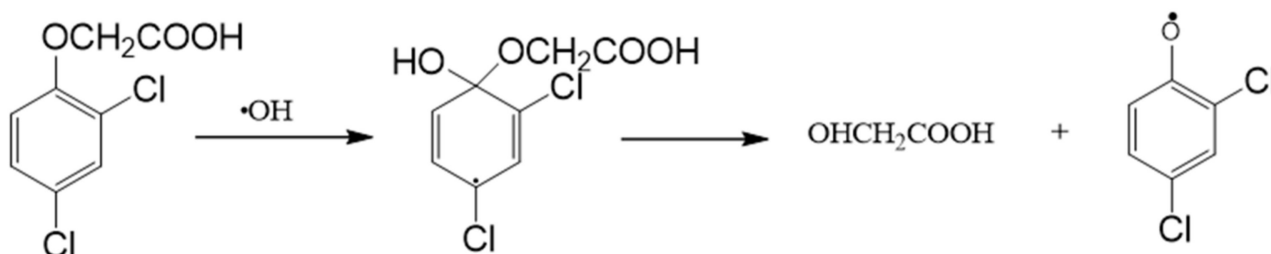


Figure 12. Carboxylic acids determined by IC during RFD (input power, 200 W; [2,4-D]₀, 1.0 mM; pH₀, 2.0).

As shown in Figure 11, glycolic acid, formic acid and oxalic acid were produced. The yields of formic acids and glycolic acid increased to the maximums within 120 min and then diminished gradually. On the other hand, the yield of oxalic acid increased smoothly

within 180 min and then declined. At 120 min, they are present with: glycolic acid at 0.31 mM, formic acid at 0.20 mM, and oxalic acid at 0.13 mM (Figure 12).

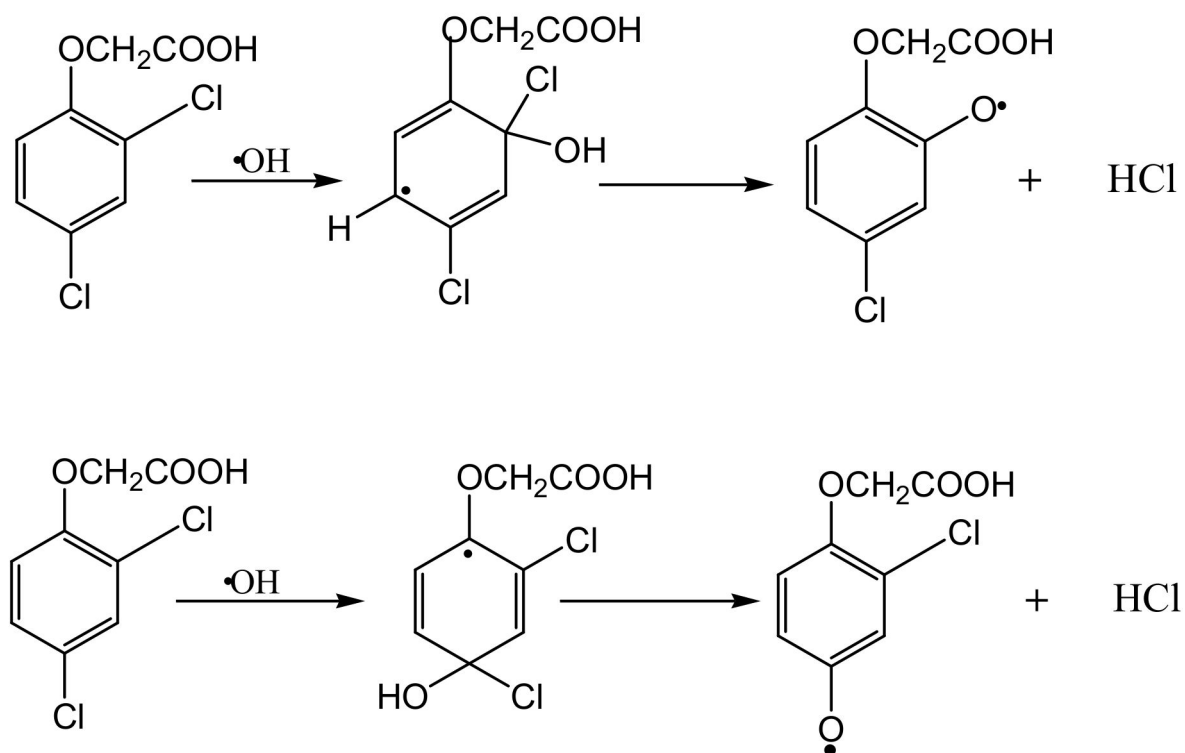
Figure 12 shows that the amount of glycolic acid accounts for almost half of the degraded 2,4-D, indicating that its formation results from the primary reaction step. Glycolic acid was formed by cleavage of ipso- $\bullet\text{OH}$ -adducts on position 1 of 2,4-D [25] (Scheme 3):



Scheme 3. Glycolic acid formation by cleavage of ipso- $\bullet\text{OH}$ -adducts on position 1 of 2,4-D.

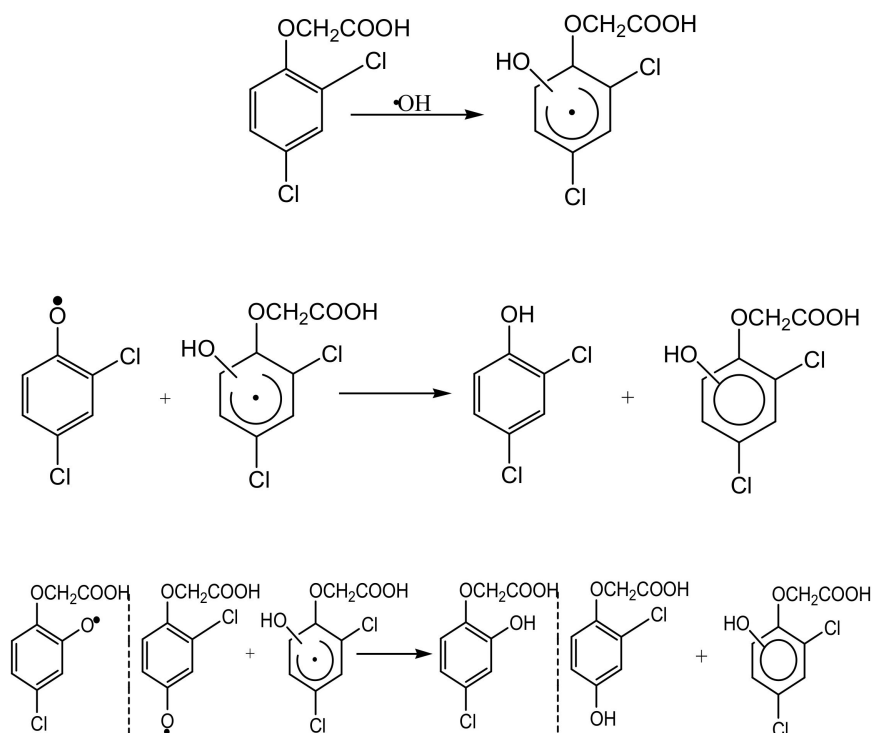
Formic and oxalic acids are common ring opening byproducts of aromatic compounds in advanced oxidation processes [12]. However, it should be noted that acetic acid observed in the ionizing radiation of 2,4-D [20] was not detected in the present investigation. This may be because the retention time of acetic acid is very close to that of glycolic acid in IC.

The formation of chloride ion (Cl^-) was attributed to the addition of $\bullet\text{OH}$ on the position of 2 or 4, followed by the fast elimination of HCl [20] (Scheme 4):



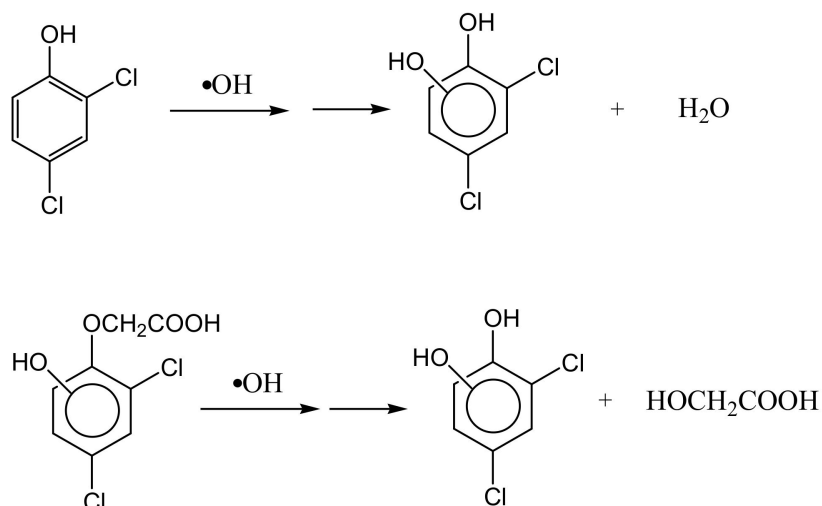
Scheme 4. Formation of chloride ion (Cl^-) due to the addition of $\bullet\text{OH}$ on the position of 2 or 4, followed by the fast elimination of HCl.

$\bullet\text{OH}$ radicals addition to the unsubstituted position of 2,4-D and then oxidized by phenoxyl radical to produce the hydroxylated 2,4-Ds and 2,4-dichlorophenol or chlorohydroxyphenoxyacetic acid [31] (Scheme 5):



Scheme 5. Mechanism for formation of hydroxylated 2,4-Ds, 2,4-dichlorophenol and chlorohydroxyphenoxyacetic acid.

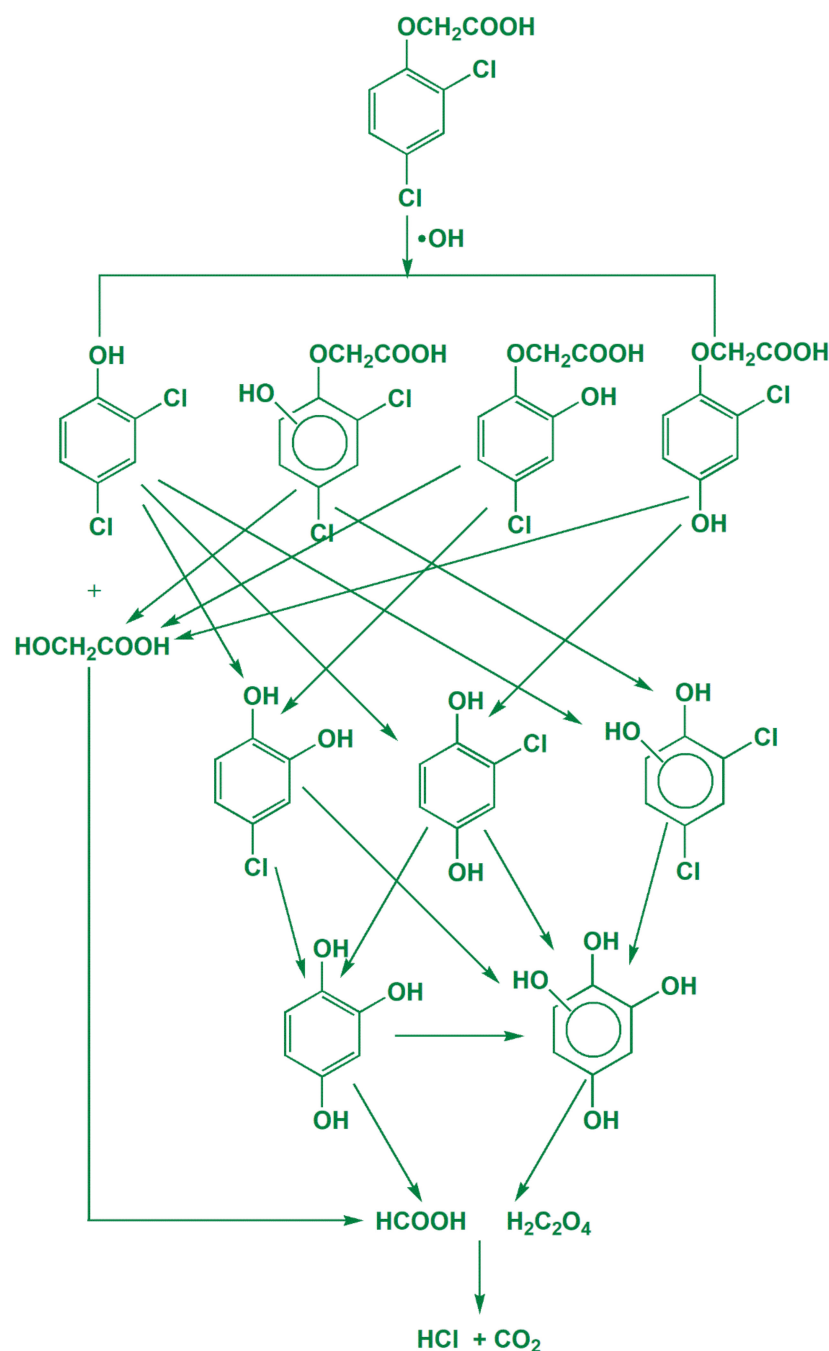
Further hydroxylation of 2,4-DCP or hydroxyl-2,4-D leads to the formation of 4,6-DCR [32] (Scheme 6):



Scheme 6. Mechanism for the formation of 4,6-DCR.

It is noted that typical phenolic byproducts such as 4-chlorocatechol, 2-chlorohydroquinone and 1, 2, 4-trihydroxybenzene commonly found in other radical processes were not observed in the present investigation, possibly because of their unstable nature [7].

Based on the above observations, the probable reaction mechanism for 2,4-D decomposition by RFD is proposed in Scheme 7.



Scheme 7. Proposed decomposition pathway for 2,4-D decomposition in RFD.

Scheme 7 shows that degradation of 2,4-D in RFD proceeds as follows: initiation of the reaction, ring destruction and oxidation of the organic acids. At the beginning stage, $\bullet\text{OH}$ radicals resulting from the RFD reacting with 2,4-D, forming the hydroxycyclohexadienyl radicals ($\bullet\text{OH}$ adducts). The $\bullet\text{OH}$ adducts formed on ipso positions subsequently undergo HCl and glycolic elimination, forming the corresponding phenoxyl radicals. The resulting phenoxyl radicals are unstable and rapidly oxidize the $\bullet\text{OH}$ adducts of the unsubstituted positions to form the corresponding phenols (2,4-DCP, 2-hydroxy-4-chloro- and 2-chloro-4-hydroxy- phenoxyacetic acids) and hydroxylated 2,4-Ds. Further hydroxylation of the aromatic ring leads to the ring cleavage to form the organic acids. The organic acids are eventually oxidized by $\bullet\text{OH}$ radicals into CO_2 and H_2O . As indicated in Figure 6,

the solution would be acidic at the end of the discharge if the 2,4-D decomposition was conducted in neutral pH. Therefore, the final product in the solution would be HCl.

3.5. Energy Yields Evaluation

Energy yields ($J_{2,4-D}$) is a significant factor in evaluating the feasibility of practical application. $J_{2,4-D}$ is calculated according to Equation (2). $J_{2,4-D}$ and reaction rate constant (k , min^{-1}) [11] of RFD, other nonthermal plasma systems and some competitive methods are summarized in Table 1.

Table 1. Energy yields for 2,4-D removal of RFD and other methods.

C_0 (mM)	Method	k	$J_{2,4-D}$	References
		min^{-1}	g/kWh	
1.0	RFD 200 W, pH ₀ 2.0	0.018	0.35	This work
1.0	RFD 200 W, pH ₀ 2.0, 0.5 mM Fe ³⁺	0.078	1.51	This work
1.0	RFD 200 W, pH ₀ 2.0, 0.5 mM Fe ²⁺	0.063	1.22	This work
10.0	RFD 200 W, pH ₀ 2.0, 20 mM H ₂ O ₂ 2,4-D, 0.5 mM Fe ³⁺	0.047	9.06	This work
0.0045	PCD over water surface, air as discharge gas (PCD/Air)		1.50	[19]
0.25	TiO ₂ photocatalysis, 125 W, 2.0g/L TiO ₂ , pH ₀ 3.3		0.76	[6]
0.22	Sonolysis, 50 W, O ₂ sparging		1.75	[9]
0.45	DBD/Ar-Fenton		8.83	[15]
0.45	DBD/Ar		3.85	[15]
0.45	DBD/Air, 200 W		0.25	[15]

Table 1 shows that the $J_{2,4-D}$ of RFD is comparable to that of sonolysis and is higher than that of TiO₂ photocatalysis. Among the nonthermal plasma systems, $J_{2,4-D}$ follows the order of DBD/Ar-Fenton \approx RFD-Fenton like > DBD/Ar > PCD/Air \approx RFD/Fe³⁺ > DBD/Air. It is shown that the $J_{2,4-D}$ of RFD/H₂O₂/Fe³⁺ is comparable to that of DBD/Ar-Fenton, the most efficient nonthermal plasma process reported. However, DBD/Ar-Fenton has to be operated in a pure noble argon atmosphere, instead of air, which would greatly increase the experimental complexity and the operation cost, indicating that RFD is not only a competitive process for 2,4-D degradation itself but also a useful tool to accelerate the Fenton-like process.

4. Conclusions

2,4-D can be efficiently degraded and dechlorinated under the action of RFD. The successive attack of •OH radicals on the benzene ring was the key step. Decreasing solution pH was favorable for the degradation. During the discharge, pH gradually decreases as HCl and organic acids are formed, and significant quantities of hydrogen peroxide are produced. Both Fe³⁺ and Fe²⁺ displayed marked catalytic effects. However, due to the reducing actions of the •OH-adducts and the hydrogen atoms, Fe³⁺ performed better than Fe²⁺, which indicates that RFD may also be used to promote the Fenton-like reactions. Major intermediate byproducts are 2,4-dichlorophenol, 4,6-dichlororesorcinol, hydroxylated 2,4-Ds, 2-hydroxy-4-chloro- and 2-chloro-4-hydroxyphenoxyacetic acids, glycolic acid, formic acid, oxalic acid and chloride ion. RFD has comparable energy yields with those of pulsed corona discharge over a water surface and sonolysis and is higher than that of TiO₂ photocatalysis, indicating that RFD is a useful process for 2,4-D decomposition.

Author Contributions: Conceptualization, Y.L.; methodology, Y.L.; software, Y.L.; validation, Y.L.; formal analysis, Y.L.; investigation, Y.L.; resources, B.S.; data curation, Y.L.; writing—original draft preparation, Y.L.; writing—review and editing, Y.L.; visualization, Y.L.; supervision, Y.L.; project administration, Y.L.; funding acquisition, Y.L. All authors have read and agreed to the published version of the manuscript.

Funding: This research was funded by the National Natural Science Foundation of China grant number [11005014, 11675031] and The APC was funded by [11005014].

Institutional Review Board Statement: Not applicable.

Informed Consent Statement: Not applicable.

Data Availability Statement: Not applicable.

Acknowledgments: The authors are thankful for the support of the National Natural Science Foundation of China (11005014, 11675031).

Conflicts of Interest: The authors declare no conflict of interest.

References

1. Available online: <https://www.invasive.org/gist/products/handbook/10.24-d.pdf> (accessed on 24 April 2001).
2. Loomis, D.; Guyton, K.; Grosse, Y.; Ghissasi, F.E.; Bouvard, V.; Benbrahim-Tallaa, L.; Guha, N.; Mattock, H.; Straif, K. Carcinogenicity of lindane, DDT, and 2,4-Dichlorophenoxyacetic acid. *Lancet Oncol.* **2015**, *16*, 891–892. [[CrossRef](#)]
3. Song, Y. Insight into the mode of action of 2,4-Dichlorophenoxyacetic acid (2,4-D) as an herbicide. *J. Integr. Plant Biol.* **2014**, *56*, 106–113. [[CrossRef](#)] [[PubMed](#)]
4. Hoover, D.G.; Borgonovi, G.E.; Jones, S.H.; Alexander, M. Anomalies in mineralization of low concentrations of organic compounds in lake water and sewage. *Appl. Environ. Microbiol.* **1986**, *51*, 226–232. [[CrossRef](#)] [[PubMed](#)]
5. Aksu, Z.; Kabasakal, E. Adsorption characteristics of 2,4-Dichlorophenoxyacetic acid (2,4-D) from aqueous solution on powdered activated carbon. *J. Environ. Sci. Health B* **2005**, *40*, 545–570. [[CrossRef](#)]
6. Trillas, M.; Peral, J.; Domènech, X. Redox photodecomposition of 2,4-Dichlorophenoxyacetic acid over TiO₂. *Appl. Catal. B Environ.* **1995**, *5*, 377–387. [[CrossRef](#)]
7. Brillas, E.; Calpe, J.C.; Casado, J. Mineralization of 2,4-D by advanced electrochemical oxidation processes. *Water Res.* **2000**, *34*, 2253–2262. [[CrossRef](#)]
8. Zona, R.; Solar, S. Oxidation of 2,4-Dichlorophenoxyacetic acid by ionizing radiation: Decomposition, detoxification and mineralization. *Radiat. Phys. Chem.* **2003**, *66*, 137–143. [[CrossRef](#)]
9. Peller, J.; Wiest, O.; Kamat, P.V. Synergy of combining sonolysis and photocatalysis in the decomposition and mineralization of chlorinated aromatic compounds. *Environ. Sci. Technol.* **2003**, *37*, 1926–1932. [[CrossRef](#)]
10. Aziz, K.H.H.; Miessner, H.; Mahyar, A.; Mueller, S.; Moeller, D.; Mustafa, F.; Omer, K.M. Degradation of perfluorosurfactant in aqueous solution using non-thermal plasma generated by nano-second pulse corona discharge reactor. *Arab. J. Chem.* **2021**, *14*, 103366. [[CrossRef](#)]
11. Aziz, K.H.H.; Miessner, H.; Mahyar, A.; Mueller, S.; Kalass, D.; Moeller, D.; Omer, K.M. Removal of dichloroacetic acid from aqueous solution using non-thermal plasma generated by dielectric barrier discharge and nano-pulse corona discharge. *Sep. Purif. Technol.* **2019**, *216*, 51–57. [[CrossRef](#)]
12. Aggelopoulos, C.A. Recent advances of cold plasma technology for water and soil remediation: A critical review. *Chem. Eng. J.* **2022**, *428*, 131657. [[CrossRef](#)]
13. Bradu, C.; Magureanu, M.; Parvulescu, V.I. Degradation of the chlorophenoxyacetic herbicide 2,4-D by plasma-ozonation system. *J. Hazard. Mater.* **2017**, *336*, 52–56. [[CrossRef](#)]
14. Singh, R.K.; Philip, L.; Ramanujam, S. Removal of 2,4-dichlorophenoxyacetic acid in aqueous solution by pulsed corona discharge treatment: Effect of different water constituents, decomposition pathway and toxicity assay. *Chemosphere* **2017**, *184*, 207–214. [[CrossRef](#)]
15. Aziz, K.H.H.; Miessner, H.; Mueller, S.; Mahyar, A.; Kalass, D.; Moeller, D.; Khorshid, I.; Rashid, M.A.M. Comparative study on 2,4-dichlorophenoxyacetic acid and 2,4-dichlorophenol removal from aqueous solutions via ozonation, photocatalysis and non-thermal plasma using a planar falling film reactor. *J. Hazard. Mater.* **2018**, *343*, 107–115. [[CrossRef](#)]
16. Maehara, T.; Miyamoto, I.; Kurokawa, K.; Hashimoto, Y.; Iwamae, A.; Kuramoto, M.; Yamashita, H.; Mukasa, S.; Toyota, H.; Nomura, S.; et al. Decomposition of methylene blue by RF plasma in water. *Plasma Chem. Plasma Process.* **2008**, *28*, 467–482. [[CrossRef](#)]
17. Amano, T.; Mukasa, S.; Honjaya, N.; Okumura, H.; Maehara, T. Generation of radio frequency plasma in high-conductivity NaCl solution. *Jpn. J. Appl. Phys.* **2012**, *51*, 978–982. [[CrossRef](#)]
18. Ji, L. *Research on Characteristics of Radio Frequency Plasma Discharge Underwater and Its Application of Azo Dyes Decomposition*; Soochow University: Suzhou, China, 2012. (In Chinese)
19. Wang, L.; Wang, J.; Lin, J.; Zhang, S.; Liu, Y. Decomposition of metronidazole by radio frequency discharge in an aqueous solution. *Plasma Proces. Polym.* **2018**, *15*, 1700176. [[CrossRef](#)]
20. Zona, R.; Solar, S.; Gehringer, P. Decomposition of 2,4-dichlorophenoxyacetic acid by ionizing radiation: Influence of oxygen concentration. *Water Res.* **2002**, *36*, 1369–1374. [[CrossRef](#)]
21. Gao, Q.; Liu, Y.; Sun, B. Characteristics of gas-liquid diaphragm discharge and its application on decolorization of brilliant red B in aqueous solution. *Plasma Sci. Technol.* **2017**, *19*, 115404. [[CrossRef](#)]

22. Harvey, A.E.; Smart, J.A.; Amis, E.S. Simultaneous spectrophotometric determination of iron (II) and total iron with 1,10-phenanthroline. *Anal. Chem.* **1953**, *26*, 1854–1856. [[CrossRef](#)]
23. Marotta, E.; Ceriani, E.; Schiorlin, M.; Ceretta, C.; Paradisi, C. Comparison of the rates of phenol advanced oxidation in deionized and tap water within a dielectric barrier discharge reactor. *Water Res.* **2012**, *46*, 6239–6246. [[CrossRef](#)]
24. Li, X.; Jenks, W.S. Isotope studies of photocatalysis: Dual mechanisms in the conversion of anisole to phenol. *J. Am. Chem. Soc.* **2000**, *122*, 11864–11870. [[CrossRef](#)]
25. Zona, R.; Solar, S.; Sehested, K.; Holcman, J.; Mezyk, S.P. OH-radical induced oxidation of phenoxyacetic acid and 2,4-Dichlorophenoxyacetic acid. Primary radical steps and products. *J. Phys. Chem. A* **2002**, *106*, 6743–6749. [[CrossRef](#)]
26. Pignatello, J.J.; Oliveros, E.; MacKay, A. Advanced oxidation processes for organic contaminant destruction based on the Fenton reaction and related chemistry. *Crit. Rev. Environ. Sci. Technol.* **2006**, *36*, 1–84. [[CrossRef](#)]
27. Wang, L.; Jiang, X.; Liu, Y. Degradation of bisphenol A and formation of hydrogen peroxide induced by glow discharge plasma in aqueous solutions. *J. Hazard. Mater.* **2008**, *154*, 1106–1114. [[CrossRef](#)] [[PubMed](#)]
28. Baxendale, J.H.; Dixon, R.S.; Stott, D.A. Reactivity of hydrogen atoms with Fe^{3+} , FeOH^{2+} and Cu^{2+} in aqueous solutions. *Trans. Faraday Soc.* **1968**, *64*, 2398–2401. [[CrossRef](#)]
29. Assadi, A.A.; Bouzaza, A.; Soutrel, I.; Petit, P.; Medimagh, K.; Wolbert, D. A study of pollution removal in exhaust gases from animal quartering centers by combining photocatalysis with surface discharge plasma: From pilot to industrial scale. *Chem. Eng. Processing Process Intensif.* **2017**, *111*, 1–6. [[CrossRef](#)]
30. Buxton, G.V.; Greenstock, C.L.; Helman, W.P.; Ross, A.B. Critical-review of rate constants for reactions of hydrated electrons, hydrogen-atoms and hydroxyl radicals ($\bullet\text{OH}/\bullet\text{O}^-$) in aqueous-solution. *J. Phys. Chem. Refer. Data* **1988**, *17*, 513–886. [[CrossRef](#)]
31. Quint, R.M.; Park, H.R.; Krajnik, P.; Solar, S.; Getoff, N.; Sehested, K. γ -radiolysis and pulse radiolysis of aqueous 4-chloroanisole. *Radiat. Phys. Chem.* **1996**, *47*, 835–845. [[CrossRef](#)]
32. Albarrán, G.; Mendoza, E. Radiolytic oxidation and degradation of 2,4-dichlorophenol in aqueous solutions. *Environ. Sci. Pollut. Res.* **2019**, *26*, 17055–17065. [[CrossRef](#)]